Approaches to Adaptive-Optic Correction for Aero-Optics Based on the Proper Orthogonal Decomposition

Shaddy Abado[a], Stanislav Gordeyev[b], Eric Jumper[c]

Institute for Flow Physics and Control, University of Notre Dame,

Notre Dame, IN, 46556 USA

Fax: 574-631-8355

[a] Corresponding author
E-mail: sabado@nd.edu

[b] Research Associate Professor, Department of Aerospace and Mechanical Engineering
E-mail: sgordeye@nd.edu

[c] Professor, Department of Aerospace and Mechanical Engineering
E-mail: ejumper@nd.edu

ABSTRACT

Methods for extracting the spatial and temporal requirements of deformable mirrors in adaptive-optic systems are presented. These systems are required to mitigate the aberrations present in wavefronts due to aero-optical turbulence over the pupil of a turret on the side of an airborne platform. The derived methods make use of the two-dimensional Proper Orthogonal Decomposition (POD) to characterize the spatial and temporal frequencies of in-flight measured data from the Airborne Aero-Optics Laboratory (AAOL). Such information is useful in designing adaptive-optic correction approaches to mitigate the deleterious effects of a laser propagated through a turbulence flow-field. A wavefront dataset (Azimuth 157 deg and Elevation 40 deg) from the AAOL is analyzed using the derived technique. For this dataset, the laser beam propagates through a fully-separated flow. The paper concludes with a discussion that points out the usefulness of the derived technique in characterizing the aero-optical disturbances as a function of viewing angles.

Keywords: Aero-optics, Adaptive-optics, Proper Orthogonal Decomposition, Airborne Aero-Optics Laboratory, Wavefront Sensor, Deformable Mirror, Hemisphere-on-Cylinder Turret, Flat Windowed Turret

1. INTRODUCTION

Aero-optics[1] refers to the aberrations imposed on an otherwise-planar wavefront of a laser propagated through near-field turbulence in flows over and around a turret on an airborne laser platform. The magnitude of these aberrations can be quite large depending on the flight altitude and Mach number as well as the pointing direction which is commonly described with the azimuthal (AZ) and elevation (EL) angles of the outgoing beam, referenced to the angle of the flight relative wind (i.e., Az 0.0^o, El 0.0^o being directly into the flight direction).[2] The magnitude of these aberrations can be sufficiently large to greatly reduce the system's useful field of regard. Adaptive-optics[3], which attempts to place a conjugate wavefront on the beam before it propagates through the turbulence, could theoretically reopen the field of regard; however, both the spatial and temporal frequencies contained in the aberrations make conventional adaptive-optic approaches minimally effective and often cause worse aberrations than are present with no "correction."

Until recently, the only available experimental wavefront measurements of aero-optical disturbances around airborne turrets have come from wind-tunnel experiments and numerical simulations. In addition, no flight-tests were available to

verify if the aero-optical disturbances are also present to the same degree in flight conditions. To address this need, an Airborne Aero-Optical Laboratory (AAOL) was designed, and a series of experiments were carried[4].

An initial analysis of the AAOL dataset was presented in our previous paper[5] where a four beam Malley probe technique was derived and applied to two wavefront datasets to determine the 2-D velocity distributions across the beam's aperture. The research described in this paper expands this initial research by exploring new analysis techniques for analyzing and manipulating the in-flight measured wavefronts. This technique begins with applying the two-dimensional Proper Orthogonal Decomposition[6] (POD) to the in-flight measured datasets to characterize the nature of the aberration field around the airborne turret due to flow structures convecting over the aperture. The analysis techniques presented in this paper for determining the basic character of the aberrations were also shown to be helpful in determining the spatial and temporal requirements of deformable mirrors in an adaptive-optics correction system for a given turret's coordinates. In the presence or absence of flow control, this sort of information should be helpful in developing a set of simplified benchmarks and guidelines for determining the minimum requirements an adaptive-optics system needs to meet to effectively mitigate the deleterious aero-optic effects on the beam.

In order to properly describe our analysis' technique, we will first give a description of the in-flight measured dataset and the scaling laws, and then a brief overview of POD analysis technique. Finally, the POD parameters (temporal coefficients and spatial modes) will be linked to the adaptive-optics system required specifications.

2. IN-FLIGHT MEASURED DATASET AND APPLICATION FLIGHT SCENARIO

The technique described in this paper can be applied to the time series of wavefronts on all of the AAOL data, but as an example of its application, one particular dataset will be used. This dataset is backward looking direction with azimuth and elevation of 157^o and 40^o, respectively. For this pointing direction, a dataset of wavefronts for a flight at $15\,kft$ altitude and a Mach number of 0.4 was chosen. This viewing angle represents a case where the flow is separated behind the turret and is dominated by the large coherent structures of the shear layer. At $15\,kft$ the air density was $\sim 0.7\ {}^{kg}\!/_{m^3}$, and the speed of sound was $\sim 322\ {}^{m}\!/_{s}$ so that the freestream velocity was $U_\infty \sim 129\ {}^{m}\!/_{s}$. The wavefront data was collected with high-speed Shack-Hartmann[3] wavefront sensor framing at $20\,kHz$ and the dataset contained 9189 frames of $30x29$ sub-apertures laid out in a rectangular array.

It is common to present wavefront results in non-dimensional quantities for easy scaling to any relevant flight conditions and turret configurations different than those experienced during the in-flight data collection. As such, the optical path difference (OPD), spatial frequency, and temporal frequency presented in this paper were first non-dimensionalized similar to the scaling laws proposed in Refs 7 and 8. Then, for the purpose of this study, we chose to re-scale the AAOL measurement to an application flight at $25\,kft$, Mach of 0.5, turret diameter of $D_t = 1\,m$, aperture diameter of $D_{Ap} = D_t \big/ 3 = \frac{1}{3}\,m$, and $1\,\mu m$ wavelength laser.

3. APPLICATION OF PROPER ORTHOGONAL DECOMPOSITION TO THE AAOL

It was discovered in the middle of the 20th century that turbulent flows are not completely random, but possess large-scale, spatially-correlated, *coherent structures* which appear repeatedly in more or less the same form[9]. Coherent structures can generally be defined as regions of organized, energetic, motion which may be dominant in determining the overall characteristics of the flow-field. In this study, an analysis of the coherent structures can provide an improved understanding of the different aspects of the aero-optical disturbances around airborne turrets.

There are various methods to predict and identify coherent structures in experimental dataset. In this study, the POD technique was used mostly due to its optimality, objectivity, and lack of bias. This choice is supported by the fact that there is a lack of a precise definition for a coherent structure. An additional reason to prefer the POD analysis over other decompositions, such as Fourier decomposition, is that coherent structures in turbulent flows are quite finite in their spatial extent and localized, while other decompositions could be of an infinite spatial extent; therefore they are not suited to analyze coherent structures[10-12].

The POD is a linear procedure, which decomposes a set of data signals (snapshots) which are varying in both space and time into the *optimal* linear basis (modes) possible. Hence, it can find a new set of dimensions that better capture the variability of the data. The POD was developed by several people and can be traced back to Karhunen[13] and Loève[14]. A comprehensive discussion of the POD technique can be found in Ref. 6. In the context of turbulence, the POD was introduced by Lumley[15]. The nice thing about using POD is that it separates the modal structures by their contribution to the overall aero-optical "energy" or OPD_{rms}^2, providing the quantitative measure of the aberrations due to that mode[7].

The POD analysis splits the spatiotemporal field into a series of statistically-correlated, stationary, spatial patterns (spatial modes), $\varphi_n(x,y)$, and corresponding time-dependent coefficients (temporal coefficients), $a_n(t)$. This split simplifies the interpretation of the dominant wavefront structures and their characteristics. Based on this, the temporal coefficients and the spatial modes can be used to reconstruct the original in-flight measured wavefronts-field, $OPD_n^{Org}(t,x,y)$. The reconstructed wavefronts-field can be expressed as

$$OPD_n^{Rec}(t,x,y) = \sum_{i=1}^{n} a_i(t) \cdot \varphi_i(x,y) \tag{1}$$

where n is the number of modes used to reconstruct the wavefronts dataset.

The residual error of comparing the reconstructed wavefronts dataset and the original in-flight measured wavefronts dataset can be defined as,

$$OPD_n^{Error}(t,x,y) = OPD^{Org}(t,x,y) - OPD_n^{Rec}(t,x,y) \tag{2}$$

An initial application of the POD to the AAOL data was presented in Ref. 5 where it was shown that the overall amplitude of the temporal coefficients, and hence their relative contribution to the total "energy", decreases as the mode number increases. There would be no reason to expect a priori that the temporal coefficients would have the same frequency as the original dataset. However, both the in-flight measured OPD's dataset, $OPD^{Org}(t,x,y)$, and the temporal coefficients are driven by the same mechanism within the flow, namely the largest, coherent structures. Therefore, the wavefronts' time evolution characterization can be identified in the temporal frequency spectra of the POD temporal coefficients.

Let $\Psi_n(f_t)$ be the temporal power spectral density (PSD) of POD temporal coefficient $a_n(t)$. Then, the PSDs of the sum of temporal coefficients starting from the first mode until mode n, $\Psi_{\sum_{i=1}^{n} a_i(t)}$, are shown in Figure 1 for $n = 1,2,3,4,10$, and 20. Each PSD is compared to the PSD of the sum of all temporal coefficients, $\Psi_{\sum_{i=1}^{N_{total}} a_i(t)}$. As expected, it can be clearly noticed that as more temporal coefficients are added, the better that $\Psi_{\sum_{i=1}^{n} a_i(t)}$ resembles $\Psi_{\sum_{i=1}^{N_{total}} a_i(t)}$. In addition, the low-order temporal coefficients reflect the low temporal frequency content of the wavefronts disturbances, while the high-order temporal coefficients reflect the high temporal frequency content of the

wavefronts disturbances. Furthermore, the sum of the first four temporal coefficients is sufficient to resolve the broad-band hump which indicates the presence of large-scale coherent structures due to the presence of a shear layer[5, 16]. This shear layer develops from the separation point on the turret and dominates the separated flow at large aft-looking viewing angles, similar to the angle presented here.

It was shown in Ref. 5 that first four spatial modes reflect the presence of large-scale coherent structures. Similarly, we can conclude based on Figure 1 that it takes four temporal coefficients to resolve the broad-band hump energy-wise. In addition, the convective nature of these four modes, which was presented in our previous paper[5], is consistent with the local phase convective velocity mapping which also was presented in the same paper and was performed over the same broad-band hump frequency range.

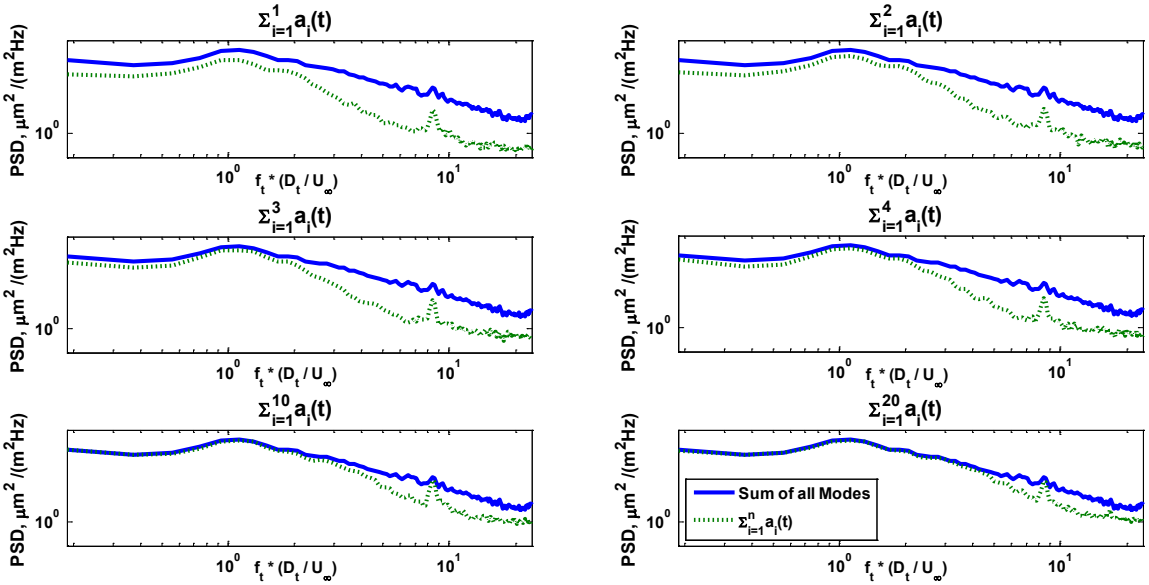

Figure 1. Power Spectral Density of $\Psi_{\sum_{i=1}^{n} a_i(t)}$ for $n = 1,2,3,4,10$, and 20.

4. AN APPROACH TO SPATIAL AND TEMPORAL FREQUENCIES FOR AERO-OPTICS CORRECTION

The results of the previous section indicate that when correcting for aero-optical disturbances, the primary correction should account for the low-order modes as they contain the most dominant and energetic spatial and temporal features of the flow-field. It can also be shown that the efficiency of the adaptive-optics correction depends upon various

parameters[3], such as the type of spatial correction applied, the resolution of the spatial correction, and the correction-update rate. The spatial and temporal requirements to mitigating aero-optical aberrations using adaptive-optics system, and the influence of the systems' parameters on its performance, will be analyzed and discussed further in this section.

4.1 Spatial Requirements

The spatial resolution of the adaptive-optics correct is limited by the deformable mirror which is used to imprint the conjugate wavefront phase onto the optical beam. In our previous paper[5], it was shown that it is possible to characterize the spatial extent of the coherent structures and to obtain the specific spatial requirements in the flow and cross-flow directions by calculating the correlation length of each spatial POD mode. For the purpose our analysis, the correlation length was defined as the location of the auto-correlation function's first minimum[17-18].Denoting the correlation length of the spatial POD mode n as $C.L.^n$, then its spatial frequency, f_s^n, can be defined as,

$$f_s^n = 1/C.L.^n \tag{3}$$

and the number of periods of aberrations per aperture, $1/Aperture$, can be defined as

$$1/Aperture = D_{Ap} \cdot f_s^n \tag{4}$$

A plot of the POD mode number versus the number of periods of aberrations per aperture in the streamwise and spanwise directions for the first 200 POD modes is shown in Figure 2(left). The spatial Nyquist frequency, which sets the spatial limit over the smallest structure size that can be resolved, is also plotted (dashed line). Based on this figure, it can be noticed that for a constant POD mode number, the number of periods of aberration per aperture in the streamwise direction is larger than the number of periods of aberration per aperture in the spanwise direction. This indicates that the streamwise correlation lengths are smaller than the spanwise correlation lengths. Furthermore, it can be noticed that the number of periods of aberration per aperture curve increases as the POD modes number increases and asymptotically converge to the spatial Nyquist frequency curve; therefore, the analysis presented here concentrates only on POD mode numbers lower than 200. These observations coincide with the Ref. 5 observation, that is, higher POD modes contained higher spatial frequencies.

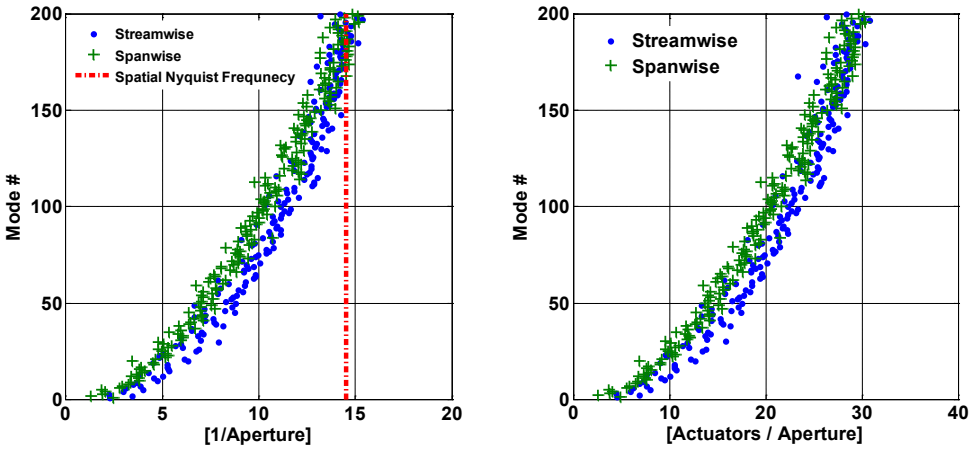

Figure 2. Spatial requirements based on the first 200 POD modes: (left) POD mode number versus the number of periods of aberrations per aperture; (right) POD mode number versus the number of required actuators per aperture.

Now, when the coherent structures have been identified based on the POD technique and characterized by their correlation lengths, it is possible to determine the spatial requirement of an adaptive-optics system for aero-optical disturbances. To analyze the spatial requirement of the system, it is necessary to define the number of required actuators per aperture parameter, $Actuators/Aperture$, as:

$$N_{\mathrm{Re}q}^{n} = 2 \cdot D_{Ap} \cdot f_{s}^{n} \tag{5}$$

This parameter is the minimum number of deformable mirror actuators per turret's aperture which are required to compensate for the coherent structure of POD mode n. Based on Eq. (5), the number of required actuators per aperture can be calculated to determine the spatial requirements as a function of a mode number. A plot of the POD mode number versus the number of required actuators per aperture for the first 200 spatial POD modes is presented in Figure 2(right).

It was shown in Section 3 that it is possible to calculate the time-averaged, root-mean-squares, residual error of the reconstructed wavefronts dataset, $\overline{OPD_{rms}^{Error}}$,as a function of mode number n, where the reconstruction residual was denied in Eq. (2). Based on this, it is possible to relate the number of actuators per aperture of the deformable mirror to a correction residual error value by re-plotting Figure 2(right) where each mode number is replaced with its associate

$\overline{OPD_{rms}^{Error}}$ value, see Figure 3. As it can be seen, the correction root-mean-squares residual error decreases as the number of actuators per aperture increases. Curve fits for the streamwise and spanwise directions are shown in Figure 3. In addition, it can be seen that for a constant value of $\overline{OPD_{rms}^{Error}}$, the number of required actuators per aperture in the streamwise direction is larger than the number of required actuators per aperture in the spanwise direction. This result indicates that the adaptive-optics correction system needs to be designed based on the streamwise direction spatial structures characteristics as they contain the dominant features of the flow-field.

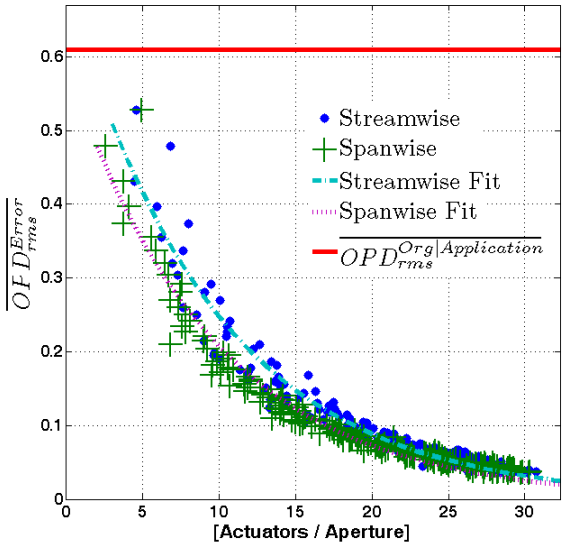

Figure 3. Time-averaged, root-mean-squares, residual wavefront error versus the number of required actuators per aperture (Application flight scenario).

Knowing the time-averaged, root-mean-squares, residual errors, it is possible to calculate the Strehl ratio[19] based on the large aperture approximation[2, 19,-20]. Assuming a $1\mu m$ wavelength laser, the Strehl ratio versus the number of required actuators per aperture for the application flight scenario is shown in Figure 4. For a number of actuators per aperture value of less than 7 the Strehl ratio almost equal to zero. This observation indicates that a spatial correction almost does not exist for this range of number of actuators per aperture. This range corresponds to the large eddies which dominate Assuming a $1\mu m$ wavelength the flow and is represented by the low-order spatial POD modes. Once these large structures are resolved, the performance of the system increases rapidly.

As the number of actuators per aperture value increases, the curves' values in Figure 4 alos increase. Curve fits to the Strehl ratio values in the streamwise and spanwise directions are shown in Figure 4. As expected, it can be noticed that as the number of deformable mirror actuators increase, more spatial structures are resolved and therefore the Strehl ratio increases.

Three main observations can be concluded from Figure 4. The first observation is that for a constant number of deformable mirror actuators per aperture, the Strehl ratio value which is based on the streamwise direction is smaller than the Strehl ratio value which is based on the spanwise direction. As an example, for a spatial correction with 15 actuators per aperture, the Strehl ratio value which is based on the spanwise direction requirements is 0.6 ($\sim 2.2 - dB$), while the Strehl ratio value which is based on the streamwise direction requirements is 0.5 ($\sim 3 - dB$). This observation reconfirms the conclusion that the system requirements which are based on the streamwise direction spatial features are stricter than the system requirements which are based on the spanwise direction spatial features.

The second observation which can be concluded is that the exponential curve fits asymptotically converge to a Strehl ratio value of 1 as the number of actuators per aperture increases; however, neither curve do not reach a Strehl ratio value of 1. The third observation is that the streamwise and spanwise curve fits converge to the same Strehl ratio value as the number of actuators per apertures increases.

The latter two observations are related to the presence of high spatial frequency structures which could not be resolved due to the spatial sampling frequency limitation of the experimental setup. In addition, for small low-frequencies, the coherent structures in the streamwise direction are more dominant than the coherent structures in the spanwise direction. However, as the spatial frequency of the coherent structures increases, the structures become incoherent in both flow directions, thus indistinguishable. Furthermore, it can be shown that small structures, which produce strong high-frequency turbulence, may not produce significant optical aberrations[21]. Despite the inaccuracy for high spatial frequency structures, our analysis is still valid to the low spatial frequency structures which dominate the flow-field.

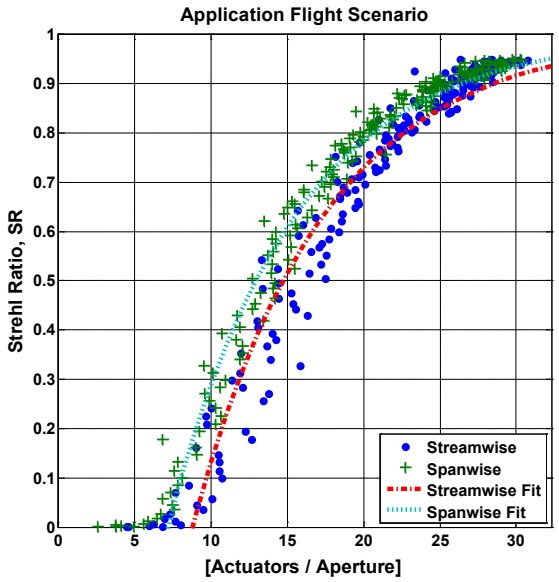

Figure 4. Strehl ratio versus the number of required actuators per aperture for an application flight scenario at Az and El of 157° and 40°.

4.2 Temporal Requirements

After analyzing the spatial requirement that the aero-optical disturbances impose on an adaptive-optics corrective system, the temporal requirements need to be analyzed. The spatial analysis, which was discussed above, assumed no time latency in applying the aero-optical correction. In this section, a perfect spatial adaptive-optic correction is assumed to investigate the effects of time latency, temporal sampling frequency, and loop gain on the corrective adaptive-optics system's performance.

As it was discussed in Section 3, the temporal coefficients of the POD analysis contain the temporal characteristics of the aero-optical disturbances. Based on these temporal coefficients, it is possible to simulate the response of a close-loop, conventional adaptive-optics system to disturbances by applying a filter in the frequency domain. The response of the close-loop control system to disturbances in the frequency domain can be considered to be a function of F_S, the discrete-time sampling frequency, β, the loop gain, and Δt, the net latency of the control system. If each temporal coefficient contains different spectral features, then applying the filter to each temporal coefficient will reject different spectral content from each mode. A summary of this correction procedure is available in Ref. 22.

To demonstrate the effects of varying the three closed-loop system's parameters (F_S , β , and Δt) on the adaptive-optics system performance, it is possible to perform a number of simulations to compare their influences on the Strehl ratio. The first comparison was performed to assess the relationship between the Strehl ratio and the loop gain for four values of 0.25, 0.5, 0.75 and 1 frame latencies. For each value of frame latency, four temporal sampling frequencies were tested. The results of this simulation are presented in Figure 5 for an application flight scenario.

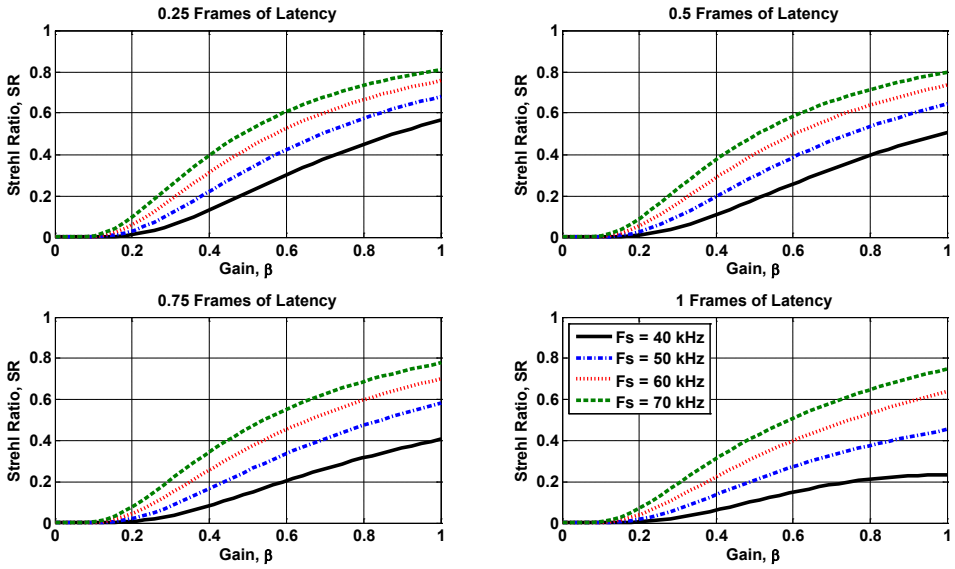

Figure 5. Strehl ratio versus loop gain for: 0.25, 0.5, 0.75 and 1 frames of latency for an application flight scenario at Az and El of 157^o and 40^o.

It can be concluded from Figure 5 that for a constant time latency value, the system's performance improves as the temporal sampling frequency increases. It can also be concluded that for a constant temporal sampling frequency value, the system's performance improves as the time latency decreases.

A similar simulation to the one presented above in Figure 5 can be repeat to assess the relationship between the Strehl ratio and the loop gain for four values of temporal sampling frequencies of 40 kHz, 50 kHz, 60 kHz, and 70 kHz. For each value of temporal sampling frequency, four frames of latency values were tested. The results of this simulation are presented in Figure 6 for an application flight scenario.

The plots in Figure 6 agree with the conclusions of Figure 5. For a constant temporal sampling frequency value, the system's performance improves as the time latency decreases. It can also be concluded that for a constant time latency

value, the system's performance improves as the temporal sampling frequency increases. Furthermore, as the temporal sampling frequency increases, the influence of decreasing the time latency on the Strehl ratio value decreases. The latter observation indicates that increasing the temporal sampling frequency of the system could lead to larger improvements in the system's performance than decreasing the time latency of the system.

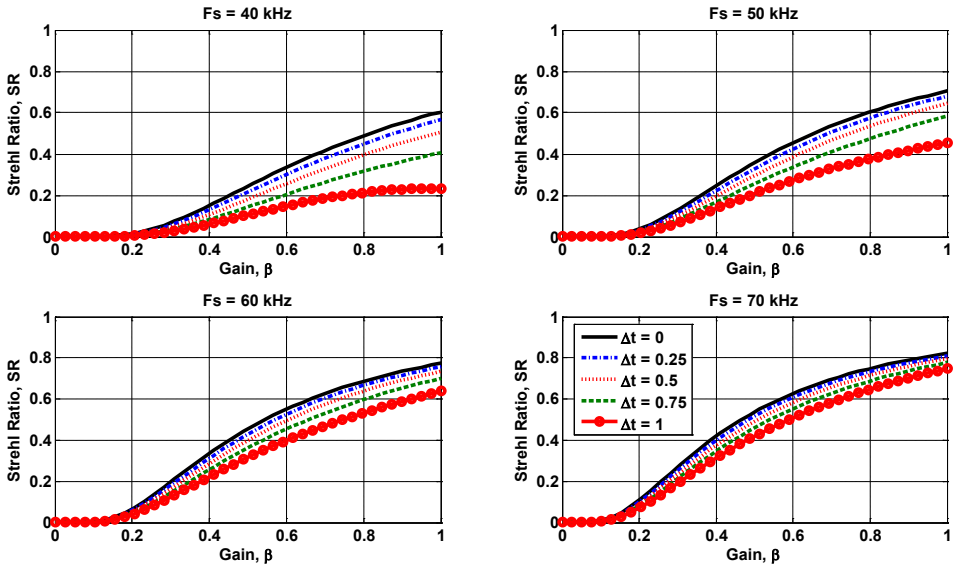

Figure 6. Strehl ratio versus loop gain for: 40 kHz, 50 kHz, 60 kHz, and 70 kHz temporal sampling frequency for an application flight scenario at Az and El of 157° and 40°.

4.3 Combining the Spatial and Temporal Requirements

In the previous two sub-sections, the spatial and temporal requirements were analyzed separately. In this sub-section, the effect of combining the two requirements is analyzed.

Let $\sigma^2_{Spatial}$ denote the spatial residual variance, the $\sigma^2_{Temporal}$ denote the temporal residual variance and assume that the two residual variances are independent, then the total wavefront error variance, σ^2_{Total}, can be expressed as,

$$\sigma^2_{Total} = \sigma^2_{Spatial} + \sigma^2_{Temporal} \tag{6}$$

Therefore, using the large-aperture approximation[2], the total Strehl ratio, SR_{Total}, can be calculated as,

$$SR_{Total} = SR_{Spatial} \cdot SR_{Temporal} \tag{7}$$

Based on the conclusions of Section 4.1, the adaptive-optics system needs to be designed based on the requirement of the spatial structures in the streamwise direction. This requirement was set based on the observation that the streamwise direction contains the dominant features of the flow-field. The exponential fit function from Figure 4 can be used to express the spatial residual variances. For the temporal residual variances, a corrective adaptive-optics system with zero time latency and 0.5 loop gain will be assumed. The total Strehl ratio as function of temporal sampling frequency for 10, 15, 20, 25, and ∞ deformable mirror actuators per aperture is shown in Figure 7. Here, ∞ actuators per aperture represent a perfect spatial correction case.

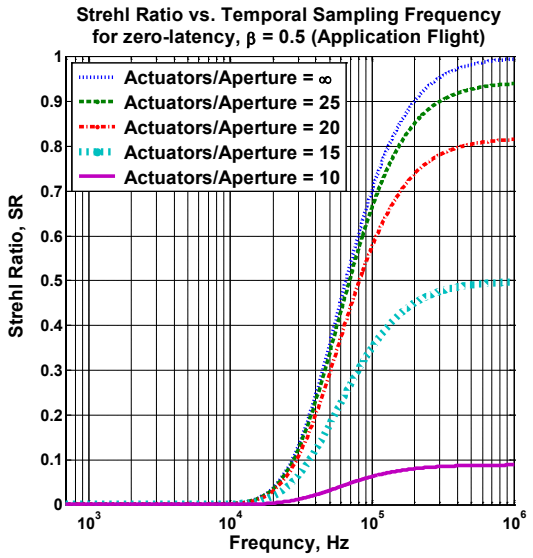

Figure 7. Total Strehl ratio versus temporal sampling frequency for: 10, 15, 20, 25, and ∞ deformable mirror actuators per aperture at for an application flight scenario at Az and El of 157° and 40°.

Similar to the conclusions of the previous sub-sections, it can be concluded from Figure 7 that the overall performance of the adaptive-optics system improves as the number of actuators per aperture increases. It can also be concluded that for a constant temporal sampling frequency value, the Strehl ratio increases more rapidly as the number of actuators per aperture increases; however, after a specific number of actuators per aperture, the increase in the total Strehl ratio value becomes less rapid and closer to the theoretical case of a perfect spatial correction. An example of this can be shown by evaluating the total Strehl ratio values at 200 kHz temporal sampling frequency. For the viewing angle considered in this paper, it can be seen that increasing the number of actuators from 10 to 15 actuators per aperture increases the total Strehl ratio value by 37%; however, increasing the number of actuators from 20 to 25 actuators per aperture increases

the total Strehl ratio value by only 10%. These are encouraging results which indicate that a modest improvement in the system's spatial resolution could result in a significant improvement in the overall system's performance. Nonetheless, there exists a spatial resolution limit value where, once it is surpassed, an increase in the system's spatial resolution will not correspond to a significant increase in the system's performance. These results can be associated with the fact that the low spatial frequency structures produce significant optical aberrations; therefore, a small addition of actuators could result in a significant improvement in the system's capability to resolve these structures. Conversely, the large spatial frequency structures may not produce significant optical aberrations; therefore, small additions of actuators will not result in a significant improvement in the system's performance.

The results of this sub-section confirm the assumption that the dominant system requirements are mostly set by the temporal frequencies of the aero-optical disturbances, and, in lesser degree, by their spatial requirements. For example, based on Figure 7, if a deformable mirror with a spatial resolution of 25 actuators per aperture and a theoretical case of zero-latency is used to mitigate the aero-optical aberrations at application flight scenario, then a 150 kHz temporal sampling frequency would be necessary to achieve a 0.8 (~0.96 -dB) Strehl ratio. However, if the same number of actuators per aperture is used, but the value of time latency increases, then the system's performance for the same temporal sampling frequency is expected to decrease.

5. CONCLUSION

The research reported in this paper involved the application of the two-dimensional Proper Orthogonal Decomposition to *in-flight* measured wavefronts from a wavefront sensor on board the University of Notre Dame's Airborne Aero-Optics Laboratory (AAOL). The primary goal of this research was to develop alternative approaches of characterizing the spatial and temporal frequency requirements for future adaptive-optic correction systems that are part of the beam-control system onboard airborne laser systems to mitigate the deleterious effects of the lasers traversing through the turbulence.

It should be emphasized that the analysis presented in this paper is based on the assumption that the dominant, characteristic, coherent structures propagate in the streamwise direction; therefore, it is sufficient to analyze one-

dimensional slices in the streamwise and spanwise directions to fully characterize the spatial requirements of the adaptive-optics system.

It can be shown that the flow topology characteristics around the airborne turret, and consequently the adaptive-optics system requirement, are viewing-angle-dependent[21]; therefore, to fully characterize the adaptive-optics system's requirement for an airborne turret, an analysis of the system's requirements for different viewing angles is necessary. This analysis will be addressed in future research papers[23].

ACKNOWLEDGMENTS

These efforts were funded by the High Energy Laser - Joint Technology Office (HEL-JTO) and administered through the Air Force Office for Scientific Research (AFOSR) under Grant Number FA9550-07-1-0574. The U.S. Government is authorized to reproduce and distribute reprints for governmental purposes notwithstanding any copyright notation thereon.

REFERENCES

[1] Jumper, E. J., & Fitzgerald, E. J. (2001). Recent advances in aero-optics. *Progress in Aerospace Sciences, 37*(3), 299-339.
[2] C. Porter, S. Gordeyev, M. Zenk and E. Jumper, "Flight Measurements of the Aero-Optical Environment around a Flat-Windowed Turret", *AIAA Journal*, Vol. **51**, No. 6, Jun. 2013, pp. 1394-1403.
[3] Tyson, R. K. (1998). Principles of adaptive optics (2nd ed.). Boston: Academic Press.
[4] E.J. Jumper, M. Zenk, S. Gordeyev, D. Cavalieri and M.R. Whiteley, "Airborne Aero-Optics Laboratory", *Journal of Optical Engineering*, **52**(7), 071408, 2013.
[5] Abado, S., Gordeyev, S., & Jumper, E. J. (2013). Approach for two-dimensional velocity mapping. *Optical Engineering, 52*(7), 071402-1-071402-11.
[6] Chatterjee, A. (2000). An introduction to the proper orthogonal decomposition. Current Science, 78(7), 808-817.
[7] Goorskey, D. J., Drye, R., & Whiteley, M. R. (2012). Spatial and temporal characterization of AAOL flight test data. Acquisition, Tracking, Pointing, and Laser Systems Technologies XXVI, Baltimore, Maryland. , SPIE Proceedings Vol. 8395-839509.
[8] Gordeyev, S., & Jumper, E. J. (2010). Fluid dynamics and aero-optics of turrets. *Progress in Aerospace Sciences, 46*(8), 388-400.
[9] Davidson, P. A. (2004). *Turbulence : An introduction for scientists and engineers*. New York: Oxford University Press.
[10] Aubry, N., Holmes, P., Lumley, J. L., & Stone, E. (1988). The dynamics of coherent structures in the wall region of a turbulent boundary-layer. *Journal of Fluid Mechanics, 192*, 115-173.
[11] Berkooz, G., Elezgaray, J., Holmes, P., Lumley, J., & Poje, A. (1994). The proper orthogonal decomposition, wavelets and modal approaches to the dynamics of coherent structures. *Applied Scientific Research, 53*(3-4), 321-338.
[12] Tritton, D. J. (1988). *Physical fluid dynamics* (2nd ed.). New York: Oxford University Press.

[13] Karhunen, K. (1946). Zur spektraltheorie stochastischer prozesse. *Ann. Acad. Sci. Finnicae, Ser. A, 1*, 34.
[14] Loève, M. M. (1955). *Probability theory*. New Jersey: Princeton: Van Nostrand.
[15] Lumley, J. L. (1970). *Stochastic tools in turbulence*. New York: New York, Academic Press.
[16] Siegenthaler, J. P., Gordeyev, S., & Jumper, E. J. (2005). Shear layers and aperture effects for aero-optics. 36th AIAA Plasmadynamics and Lasers Conference, Toronto, Canada. , AIAA Paper 2005-4772.
[17] Mela, K., & Louie, J. N. (2001). Correlation length and fractal dimension interpretation from seismic data using variograms and power spectra. Geophysics, 66(5), 1372-1378.
[18] S. Gordeyev, T. Hayden and E. Jumper, "Aero-Optical and Flow Measurements Over a Flat-Windowed Turret", *AIAA Journal*, vol. **45**, No. 2, pp. 347-357, 2007.
[19] T. S. Ross," Limitations and applicability of the Maréchal approximation, " Appl. Opt. 48(10), 1812–1818 (2009)
[20] C. Porter, S. Gordeyev and E. Jumper, **"**Large-Aperture Approximation for Not-So-Large Apertures", *Journal of Optical Engineering*, **52**(7), 071417, 2013.
[21] Rennie, R. M., Duffin, D. A., & Jumper, E. J. (2008). Characterization and aero-optic correction of a forced two-dimensional weakly compressible shear layer. *AIAA Journal, 46*(11), 2787-2795.
[22] Goorskey, D. J., Whiteley, R. M., Gordeyev, S., & Jumper, E. J. (2011). Recent AAOL in-flight wavefront measurements of aero-optics and implications for aero-optics beam control in tactical laser weapon systems. *42nd AIAA Plasmadynamics and Lasers Conference,* Honolulu, Hawaii *, AIAA Paper 2011-3282.*
[23] Abado, S., Gordeyev, S., & Jumper, E. J. Approaches to Adaptive-Optic Correction for Aero-Optics as a Function of Viewing Angles. Manuscript in preparation.